ISSN 0915-633X

NATIONAL INSTITUTE FOR FUSION SCIENCE

Superposed-Laser Electron Acceleration

T. Maruyama and S. Kawata

(Received – Nov. 25, 1991)

NIFS-133 Feb. 1992

RESEARCH REPORT
NIFS Series

NAGOYA, JAPAN

Superposed-Laser Electron Acceleration

T. Maruyama and S. Kawata

Department of Electrical Engineering,
Nagaoka University of Technology,
Nagaoka 940-21, Japan

Abstract

A new mechanism is proposed for electron acceleration by using two superposed laser beams in vacuum. In this mechanism, an electron is accelerated by the longitudinal component of the wave electric field in the overlapped region of two laser beams. Single-particle computations and analytical works are performed in order to demonstrate the viability. These results show that the electron can be accelerated well in this proposed mechanism.

Key words: particle acceleration, electron acceleration, high-energy electron, laser acceleration

Recently, a number of mechanisms [1-19] have been proposed for high energy particle acceleration. We have also proposed electron acceleration mechanisms in systems of the inverse synchrotron radiation [16,17] and the inverse bremsstrahlung [18]. In these mechanisms, a static magnetic field or a static electric field is applied so that the symmetry of the electromagnetic (EM) wave in space and time is removed and then electrons can absorb the wave energy. Without a static magnetic field or a static electric field an electron can not be accelerated by an EM wave generally in vacuum, because of the symmetry of EM wave.

In this paper we present a new mechanism [20] for an electron acceleration by using only lasers in vacuum. Figure 1 shows the mechanism proposed in this paper for the electron acceleration. In this mechanism two superposed laser beams are used in vacuum. These two beams can produce the longitudinal electric field by which electrons can be accelerated in a straight trajectory, as follows: Laser beams have the incident angle of $\pm\theta$ to the x axis and cross on the x axis. These electromagnetic waves have the same wavelength, the converse phases with each other and the same amplitude. The magnetic component of the waves is in the $x-z$ plane and the electric one is in the $x-y$ plane. In the crossing region of two lasers, the electromagnetic field is represented by the following expressions:

$$E_x = E_{y0}\sin\theta\sin[k(x\cos\theta - y\sin\theta - ct)] + E_{y0}\sin\theta\sin[k(x\cos\theta + y\sin\theta - ct)], \quad (1)$$

$$E_y = E_{y0}\cos\theta\sin[k(x\cos\theta - y\sin\theta - ct)] - E_{y0}\cos\theta\sin[k(x\cos\theta + y\sin\theta - ct)], \quad (2)$$

$$B_z = B_{z0}\sin[k(x\cos\theta - y\sin\theta - ct)] - B_{z0}\sin[k(x\cos\theta + y\sin\theta - ct)]. \quad (3)$$

On the x axis the electric component (E_y) in the y direction and the magnetic component (B_z) in the z direction are canceled out, and the electron staying on the x axis feels only the electric component (E_x) in the x direction. Therefore electrons can be accelerated by this E_x with choosing an appropriate parameter set which will be discussed below in detail. This is the mechanism which we propose. We performed numerical analyses and analytical works for the acceleration mechanism. We also discuss the radiation energy loss from the accelerated electron at the end of this paper. In

addition to the above analyses for the electron on the x axis, we also discuss the behavior of the electrons off the x axis in this paper.

The equation of motion and the energy equation for the electron moving on the x axis ($y = 0$) are

$$dP_x/dt = F_x = -eE_x - e\beta_y B_z = -eE_x, \tag{4}$$

$$dP_y/dt = F_y = -eE_y + e\beta_x B_z = 0, \tag{5}$$

$$d(mc^2\gamma)/dt = -eE_x v_x. \tag{6}$$

Here $\beta_x = v_x/c$ and $\beta_y = v_y/c$. In the half-wavelength of $0 > k(x\cos\theta - ct) > -\pi$, F_x becomes $F_x > 0$ and the electron is accelerated in the $+x$ direction. In the remaining one of $-\pi > k(x\cos\theta - ct) > -2\pi$, F_x becomes $F_x < 0$ and the electron is decelerated. Consequently we choose the optimal incident angle and radius of lasers so that the electron interacts with the lasers only in the half wavelength of $0 > k(x\cos\theta - ct) > -\pi$ in order to accelerate the electron well. The electron staying on the x axis is therefore accelerated along the x axis and the radiation energy loss is minimized.

First, we perform single-particle analyses numerically in order to demonstrate the viability of this mechanism. In these analyses, an electron has the initial speed v_{x0} in the $+x$ direction. The amplitude of the plane EM wave E_{y0} is AE_0, where A is a constant factor and $E_0 = mc^2/(\sqrt{2}e\lambda/32) = 1.157 \times 10^7/\lambda\ V/cm$; for the wavelength $\lambda = 10\mu m$, E_0 is $1.77 \times 10^{15} W/cm^2$. Table 1 shows several results of the beam diameter d, the optimal incident angle of θ, $R \equiv \gamma/\gamma_0$, the final γ and the acceleration gradient G, where γ/γ_0 is the ratio of the final relativistic factor to the initial one. These results present that the electron can be accelerated well and that the high acceleration gradient of $1 \sim 10 GeV/m$ can be attained. Here it should be noted that the crossing angle θ is rather small in order to make the interaction length long enough in this system.

We also perform an analytical estimation for the final γ and the optimal incident angle θ. In order to find the final γ we integrate the equation of motion in the x direction and the energy equation by introducing an effective β_{xe}, which is defined by $x = c\int \beta_x dt = c\beta_{xe} t$:

$$\begin{aligned}\gamma v_x &= -\frac{e}{m}\int_0^t E_x dt + \gamma_0 v_{x0} \\ &= \frac{2eE_0 \sin\theta}{kmc(1-\beta_{xe}\cos\theta)}\{-\cos[kc(\beta_{xe}\cos\theta - 1)t] + 1\} + \gamma_0 v_{x0}. \end{aligned} \tag{7}$$

$$\frac{d\gamma^2}{dt} = -\frac{2e}{mc^2} E_x \cdot \gamma v_x. \tag{8}$$

$$\begin{aligned}\gamma^2 &= \int_0^\tau \frac{d\gamma^2}{dt} dt + \gamma_0^2 \\ &= \frac{4e^2 E_{y0}^2 \lambda^2 \sin^2\theta}{\pi^2 m^2 c^4 (1-\beta_{xe}\cos\theta)^2} + \frac{4eE_{y0}\lambda\gamma_0\beta_{x0}\sin\theta}{\pi mc^2(1-\beta_{xe}\cos\theta)} + \gamma_0^2. \end{aligned} \tag{9}$$

Here τ is the time at $k(x\cos\theta - ct) = -\pi$ and is estimated by $\lambda/2c(1-\beta_{xe}\cos\theta)$. In order to estimate β_{xe} we use eq. (7) with the assumption of $\beta_{xe} = \beta_{x0}$ in the right hand side of eq. (7) and average it over τ', where $\tau' = \lambda/2c(1-\beta_{x0}\cos\theta)$. Consequently we obtain the following expression:

$$\frac{1}{\sqrt{1-\beta_{xe}^2}}\beta_{xe} = \frac{1}{c\tau'}\int_0^{\tau'} \gamma v_x dt. \tag{10}$$

$$\beta_{xe}^2 = \frac{\left(\dfrac{eE_{y0}\lambda\sin\theta}{\pi mc^2(1-\beta_{x0}\cos\theta)} + \gamma_0\beta_{x0}\right)^2}{1+\left(\dfrac{eE_{y0}\lambda\sin\theta}{\pi mc^2(1-\beta_{x0}\cos\theta)} + \gamma_0\beta_{x0}\right)^2}. \tag{11}$$

In addition, from eq. (9) the condition $d\gamma^2/d\theta = 0$ leads to the following equation for the optimal θ:

$$\cos\theta - \beta_{xe} + \frac{d\beta_{xe}}{d\theta}\sin\theta\cos\theta = 0. \tag{12}$$

For the optimal θ, β_{xe} should be also maximized as well as γ. Therefore this physical consideration leads to

$$\theta = \cos^{-1}\beta_{xe}. \tag{13}$$

In this paper we set β_{xe} in eq. (13) to $\beta_{xe}(\theta = \cos^{-1}\beta_{x0})$ for simplicity.

Figure 2 shows γ versus the amplitude factor A of the EM wave; the solid line and the dashed line are obtained by the analytical estimations for $v_{x0} = 0.999c$ and $0.99c$,

respectively. Dotts besides these lines are obtained by the single-particle computations presented above for these cases. Figure 3 also shows θ versus the initial speed $v_{x0} = c\beta_{x0}$ of the electron; the solid line and the dashed line are obtained by the analytical estimations for $A = 0.05$ and 0.1. Dotts are also obtained by the single-particle computations. These figures show that the analytical estimation can reproduce the general tendency of the numerical results and that the expressions (9), (11) and (13) being derived above present the correct scaling laws for this mechanism.

In addition to the analyses for the electrons on the x axis, we also perform numerical analysis for electrons off the x axis in order to estimate a quality of electron beam being accelerated. We compute the normalized emittance N which corresponds to the dimensions of electron beam in the phase space ($y, P_y/m_0c$). Here N is defined by the following expression:

$$N = \frac{1}{\pi} \int \frac{P_y}{m_0 c} dy. \tag{14}$$

Figure 4 shows the distribution of electrons in the phase space, and Figs.4(a), (b) and (c) show that at the normalized position of $x = 0, 1530$ and 6120, respectively. The point of $x = 0$ is the start point of electrons, the point of $x = 1530$ is at the left edge of overlapped region and the point of $x = 6120$ is at which almost all electrons pass through the acceleration region. The overlapped region is from $x = 1530$ to $x = 3060$. In this case the initial speed of electrons is $0.99c$ and electrons are distributed initially in $0 \leq | y | \leq 100$, $0 \leq | P_y/m_0c | \leq 1.225 \times 10^{-2}$ (see Fig.4(a)). Here the space coordinates x and y are normalized by $\lambda/32$. In this analysis we assume that there is no interaction between electrons because of the very low density of beam. The initial number density of electrons per unit area is $6.4 \times 10^6\ cm^{-2}$ and the electric field produced by the electrons is $5.790\ V/cm$. Therefore this assumption is valid in our parameter range. The normalized emittance N is 4.874×10^{-7}, 3.580×10^{-7} and 2.070×10^{-6} $m\text{-}rad$ at $x = 0$, 1530 and 6120, respectively. These results mean that the quality of electron beam becomes gradually degraded. Then we obtain the electrons which satisfy the following conditions in order to find the well-accelerated and collimated electron beam: at $x = 6120$, $0 \leq | y | \leq 5$, $0 \leq | P_y/m_0c | \leq 1.225 \times 10^{-2}$, $0.9 \times \gamma_m \leq \gamma \leq \gamma_m$, where γ_m is the maximum γ. In Fig.4 the hatched region near the origin shows these electrons satisfying the above conditions.

The number of these electrons are 0.92 percent of all employed in Figs.4. This result shows that electrons should be distributed inside the hatched region in Fig.4(a) initially in order to be accelerated well.

Finally we estimate the radiation energy loss from the accelerated electron staying on the x axis. Because of $E_y = B_z = 0$, the radiated power P is given by the following expression [21]:

$$P = \frac{2e^4}{3m^2c^3} \frac{\left\{\vec{E} + \frac{1}{c}\vec{v} \times \vec{B}\right\}^2 - \frac{1}{c^2}(\vec{E} \cdot \vec{v})^2}{1 - \left(\frac{v}{c}\right)^2} \tag{15}$$

$$= \frac{2e^4}{3m^2c^3} E_x^2. \tag{16}$$

By integrating this equation over the interaction time τ with the assumption of $\beta_x = \beta_{xe}$, we obtain the radiation energy loss ε.

$$\varepsilon = \frac{2e^4 E_{y0}^2 \lambda \sin^2\theta}{3m^2c^4(1 - \beta_{xe}\cos\theta)}. \tag{17}$$

For $A = 0.1, \beta_{x0} = 0.999$ and $\lambda = 10\mu m$, the radiation energy loss is $4.92 \times 10^{-4} eV$. This energy loss is quite small compared with the electron energy.

In this paper we proposed a new mechanism for electron acceleration and demonstrated its viability by numerical analyses and analytical works. This mechanism provides a high acceleration gradient, that is, possibly about $1 \sim 10 GeV/m$ or more, depending on the laser power and the pre-accelerated-electron initial energy. In addition, the trajectory of the accelerated electron which stays on the x axis in Fig.1 is entirely straight along the x axis and the radiation energy loss is negligible compared with the electron energy.

Acknowledgements

We would like to send our thanks to Dr. K. Sakai of Yamanashi University for his valuable comments on our present study. This work is partly supported by the cooperative

program of the National Institute for Fusion Science and the computations were performed in part at the computer center of the University of Tokyo.

References

[1]IEEE Trans. Plasma Sci., edited by T. Katsouleas, **PS-15**, No.2(1987).

[2]American Ins. of Phys. Conf. Proc. No. 130, eds. C. Joshi and T. Katsouleas (American Institute of Physics, New York,1985).

[3]T. Tajima and J. M. Dawson, Phys. Rev. Lett. **43**, 267(1979).

[4]P. Chen, J. M. Dawson, R. W. Huff and T. Katsouleas, Phys. Rev. Lett. **54**, 693(1985).

[5]K. Mizuno, S. Ono and O. Shimoe, Nature **253**, 184(1975).

[6]K. Mizuno, J. Pae, T. Nozokido and K. Huruya, Nature **328**, 45(1987).

[7]N. M. Kroll, P. L. Morton and M. N. Rosenbluth, IEEE J. Quantum Electron. **QE-17m**, 1436(1981).

[8]S. Sprangle and C. M. Tang, IEEE Trans. Nucl. Sci. **NS-28**, 3340(1981).

[9]A. Loeb and L. Friedland, Phys. Rev. **A33**, 1832(1986).

[10]A. Loeb, L. Friedland and S. Eliezer, Phys. Rev. **A35**, 1692(1987).

[11]R. Sugihara, S. Takeuchi, K. Sakai and M. Matsumoto, Phys. Rev. Lett. **52**, 1500(1984).

[12]Y. Nishida, M. Yoshizumi and R. Sugihara, Phys. Fluids **28**, 1574(1985).

[13]T. Katsouleas and J. M. Dawson, Phys. Rev. Lett. **51**, 392(1983).

[14]S. Takeuchi, K. Sakai, M. Matsumoto and R. Sugihara, IEEE Trans. Plasma Sci. **PS-15**, 251(1987).

[15]V. V. Apolonov, A. I. Artem'ev, Yu. L. Kalachev, A. M. Prokhorov and M. V. Fedorov, JETP Lett. **47**, 92(1988).

[16]S. Kawata, A. Manabe and S. Takeuchi, Jpn. J. Appl. Phys. **28**, L701(1989).

[17]S. Kawata, H. Watanabe, A. Manabe and H. Kuroda, Jpn. J. Appl. Phys. **29**, L179 (1990).

[18]S. Kawata, T. Maruyama, H. Watanabe and I. Takahashi, Phys. Rev. Lett. **66**, 2072 (1991).

[19]M. O. Scully and M. S. Zubairy, Phys. Rev. **A44**, 2656(1991).

[20]T. Maruyama and S. Kawata, Bulletin of 46th annual meeting of Japanese Physical Society (in Japanese), **4**, 199(1991).

[21]L. D. Landau and E. M. Lifshiftz, *The Classical Theory of Fields* (Pergamon, Oxford and Addison-Wesley 1971), 3rd ed.

Table caption

Table 1. The beam diameter d, incident angle of laser beam θ, $R \equiv \gamma/\gamma_0$, γ and the acceleration gradient G by the numerical single-particle analyses for the amplitude factor A of the EM wave and the intial electron speed $v_{x0} = c\beta_{x0}$.

Figure captions

Fig.1. A mechanism of high-energy electron acceleration by superposed laser beams in vacuum. An electron being placed on the x axis is accelerated in the $+x$ direction. Lasers have the incident angle of θ to the x axis, cross on the x axis and have the converse phases with each other. The electron is accelerated by the electric component in the x direction in the overlapped region of the two lasers during the interval of $0 > k(x\cos\theta - ct) > -\pi$.

Fig.2. The final electron relativistic factor γ versus the amplitude factor A of the EM wave. Solid and dashed lines are obtained by the analytical estimation for $v_{x0} = 0.999c$ and $v_{x0} = 0.99c$, respectively. Dotts besides these lines are obtained by the single-particle computations.

Fig.3. The optimal incident angle θ of the laser beams versus the initial electron speed $v_{x0} = c\beta_{x0}$. Solid and dashed lines are obtained by the analytical estimation for $A = 0.05$ and $A = 0.1$, respectively. Dotts besides these lines are obtained by the single-particle computations.

Fig.4. The electron distribution in the phase space ($y, P_y/m_0c$). Figures 4(a), (b) and (c) show that at $x = 0$, 1530 and 6120, respectively. The normalized emittance is 4.874×10^{-7}, 3.580×10^{-7} and 2.070×10^{-6} *m-rad* in Figs.4(a), (b) and (c), respectively. The hatched region shows the distribution of electrons which satisfy the following conditions: $0 \leq \mid y \mid \leq 5$, $0 \leq \mid P_y/m_0c \mid \leq 1.225 \times 10^{-2}$, $0.9 \times \gamma_m \leq \gamma \leq \gamma_m$ at $x = 6120$, where γ_m is the maximum γ.

Table 1

A	β_{x0}	$d[\mu m]$	$\theta[degree]$	R	γ	$G[GeV/m]$
	0.95	30.55	9.37	3.723	11.92	23.75
0.1	0.99	69.37	4.16	3.794	26.89	10.58
	0.999	220.2	1.31	3.810	85.21	3.335
	0.95	22.05	12.83	1.986	6.361	16.24
0.05	0.99	50.31	5.71	2.017	14.30	7.285
	0.999	160.7	1.81	2.024	45.26	2.300
	0.95	19.08	14.61	1.513	4.846	11.11
0.03	0.99	43.70	6.55	1.531	10.85	5.019
	0.999	138.9	2.07	1.535	34.33	1.590

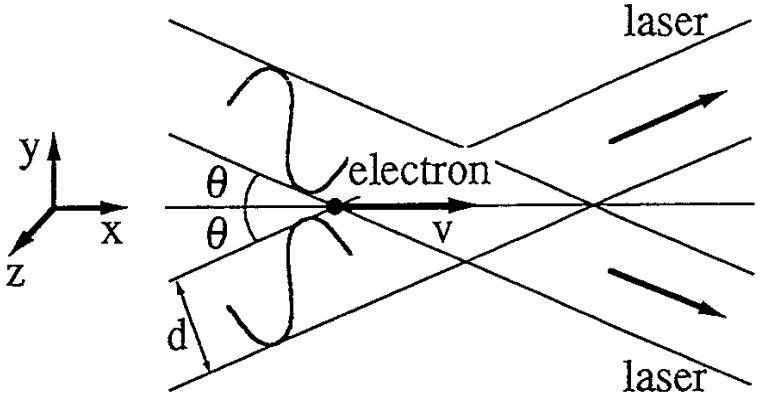

Fig.1

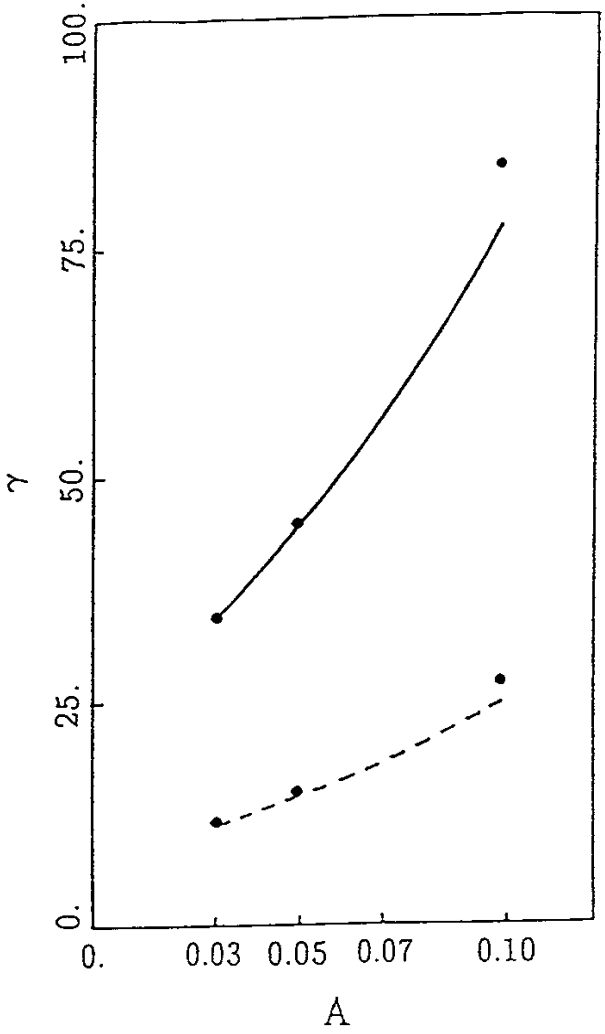

Fig.2

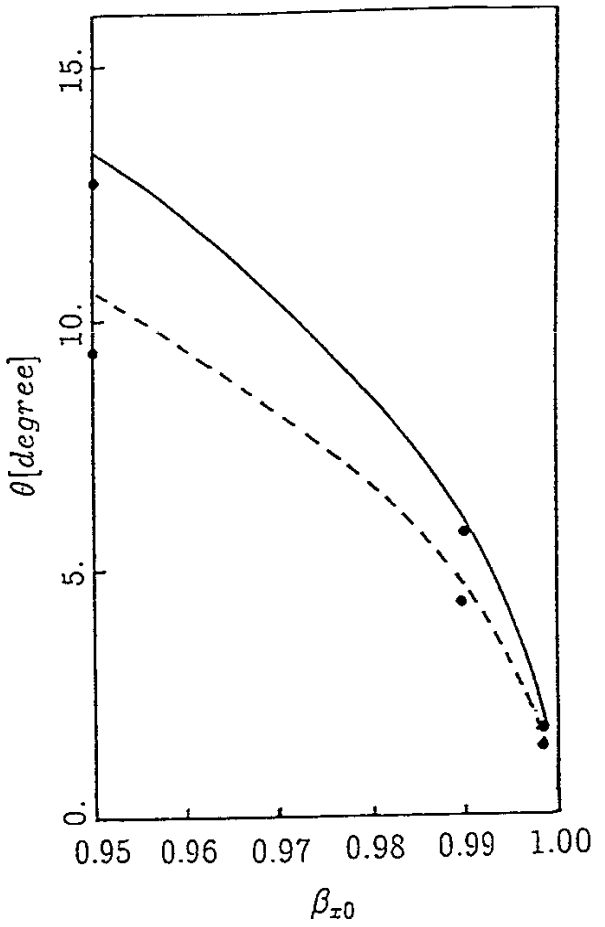

Fig.3

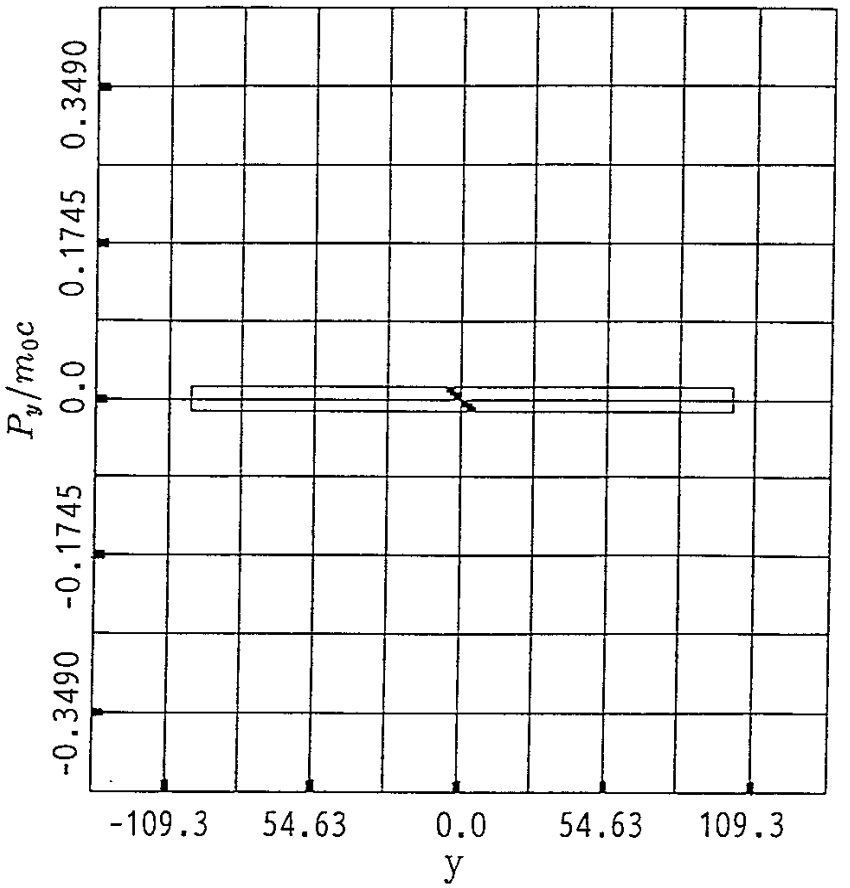

(a)

Fig.4

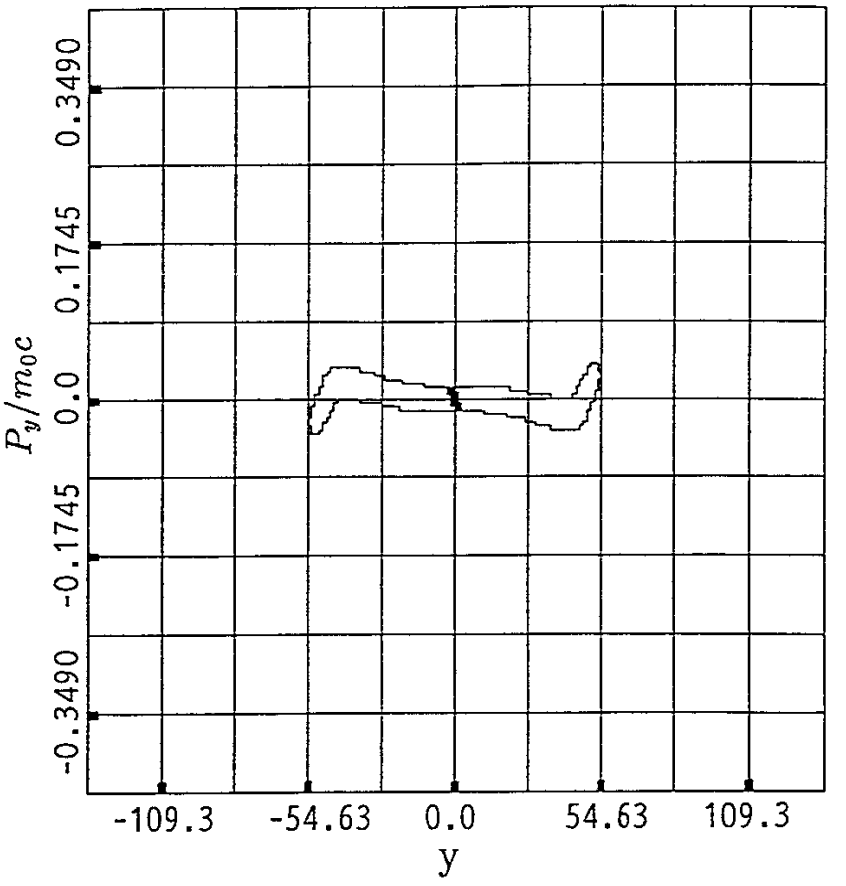

(b)

Fig.4

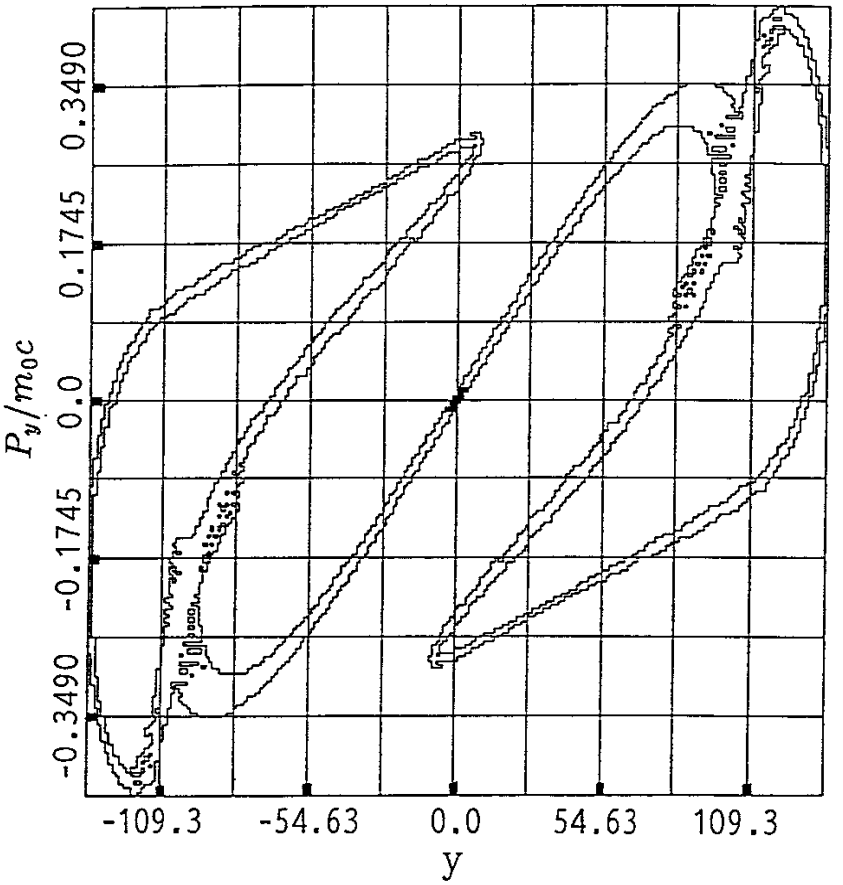

(c)

Fig.4

Recent Issues of NIFS Series

NIFS-74 T.Yamagishi, *Electrostatic Drift Mode in Toroidal Plasma with Minority Energetic Particles*, Feb. 1991

NIFS-75 T.Yamagishi, *Effect of Energetic Particle Distribution on Bounce Resonance Excitation of the Ideal Ballooning Mode*, Feb. 1991

NIFS-76 T.Hayashi, A.Tadei, N.Ohyabu and T.Sato, *Suppression of Magnetic Surface Breading by Simple Extra Coils in Finite Beta Equilibrium of Helical System;* Feb. 1991

NIFS-77 N. Ohyabu, *High Temperature Divertor Plasma Operation*; Feb. 1991

NIFS-78 K.Kusano, T. Tamano and T. Sato, *Simulation Study of Toroidal Phase-Locking Mechanism in Reversed-Field Pinch Plasma*; Feb. 1991

NIFS-79 K. Nagasaki, K. Itoh and S. -I. Itoh, *Model of Divertor Biasing and Control of Scrape-off Layer and Divertor Plasmas*; Feb. 1991

NIFS-80 K. Nagasaki and K. Itoh, *Decay Process of a Magnetic Island by Forced Reconnection*; Mar. 1991

NIFS-81 K. Takahata, N. Yanagi, T. Mito, J. Yamamoto, O.Motojima and LHDDesign Group, K. Nakamoto, S. Mizukami, K. Kitamura, Y. Wachi, H. Shinohara, K. Yamamoto, M. Shibui, T. Uchida and K. Nakayama, *Design and Fabrication of Forced-Flow Coils as R&D Program for Large Helical Device*; Mar. 1991

NIFS-82 T. Aoki and T. Yabe, *Multi-dimensional Cubic Interpolation for ICF Hydrodynamics Simulation*; Apr. 1991

NIFS-83 K. Ida, S.-I. Itoh, K. Itoh, S. Hidekuma, Y. Miura, H. Kawashima, M. Mori, T. Matsuda, N. Suzuki, H. Tamai, T.Yamauchi and JFT-2M Group, *Density Peaking in the JFT-2M Tokamak Plasma with Counter Neutral Beam Injection* ; May 1991

NIFS-84 A. Iiyoshi, *Development of the Stellarator/Heliotron Research*; May 1991

NIFS-85 Y. Okabe, M. Sasao, H. Yamaoka, M. Wada and J. Fujita, *Dependence of Au^- Production upon the Target Work Function in a Plasma-Sputter-Type Negative Ion Source;* May 1991

NIFS-86 N. Nakajima and M. Okamoto, *Geometrical Effects of the Magnetic Field on the Neoclassical Flow, Current and Rotation in General Toroidal Systems*; May 1991

NIFS-87 S. -I. Itoh, K. Itoh, A. Fukuyama, Y. Miura and JFT-2M Group, *ELMy-H mode as Limit Cycle and Chaotic Oscillations in Tokamak Plasmas;* May 1991

NIFS-88 N.Matsunami and K.Kitoh, *High Resolution Spectroscopy of H^+ Energy Loss in Thin Carbon Film;* May 1991

NIFS-89 H. Sugama, N. Nakajima and M.Wakatani, *Nonlinear Behavior of Multiple-Helicity Resistive Interchange Modes near Marginally Stable States;* May 1991

NIFS-90 H. Hojo and T.Hatori, *Radial Transport Induced by Rotating RF Fields and Breakdown of Intrinsic Ambipolarity in a Magnetic Mirror*; May 1991

NIFS-91 M. Tanaka, S. Murakami, H. Takamaru and T.Sato, *Macroscale Implicit, Electromagnetic Particle Simulation of Inhomogeneous and Magnetized Plasmas in Multi-Dimensions;* May 1991

NIFS-92 S. - I. Itoh, *H-mode Physics, -Experimental Observations and Model Theories-, Lecture Notes, Spring College on Plasma Physics, May 27 - June 21 1991 at International Centre for Theoretical Physics (IAEA UNESCO) Trieste, Italy ;* Jun. 1991

NIFS-93 Y. Miura, K. Itoh, S. - I. Itoh, T. Takizuka, H. Tamai, T. Matsuda, N. Suzuki, M. Mori, H. Maeda and O. Kardaun, *Geometric Dependence of the Scaling Law on the Energy Confinement Time in H-mode Discharges;* Jun. 1991

NIFS-94 H. Sanuki, K. Itoh, K. Ida and S. - I. Itoh, *On Radial Electric Field Structure in CHS Torsatron / Heliotron;* Jun. 1991

NIFS-95 K. Itoh, H. Sanuki and S. - I. Itoh, *Influence of Fast Ion Loss on Radial Electric Field in Wendelstein VII-A Stellarator;* Jun. 1991

NIFS-96 S. - I. Itoh, K. Itoh, A. Fukuyama, *ELMy-H mode as Limit Cycle and Chaotic Oscillations in Tokamak Plasmas;* Jun. 1991

NIFS-97 K. Itoh, S. - I. Itoh, H. Sanuki, A. Fukuyama, *An H-mode-Like Bifurcation in Core Plasma of Stellarators;* Jun. 1991

NIFS-98 H. Hojo, T. Watanabe, M. Inutake, M. Ichimura and S. Miyoshi, *Axial Pressure Profile Effects on Flute Interchange Stability in the Tandem Mirror GAMMA 10;* Jun. 1991

NIFS-99 A. Usadi, A. Kageyama, K. Watanabe and T. Sato, *A Global Simulation of the Magnetosphere with a Long Tail : Southward and Northward IMF;* Jun. 1991

NIFS-100 H. Hojo, T. Ogawa and M. Kono, *Fluid Description of Ponderomotive Force Compatible with the Kinetic One in a Warm Plasma* ; July 1991

NIFS-101 H. Momota, A. Ishida, Y. Kohzaki, G. H. Miley, S. Ohi, M. Ohnishi K. Yoshikawa, K. Sato, L. C. Steinhauer, Y. Tomita and M. Tuszewski *Conceptual Design of D-^{3}He FRC Reactor "ARTEMIS"* ; July 1991

NIFS-102 N. Nakajima and M. Okamoto, *Rotations of Bulk Ions and Impurities in Non-Axisymmetric Toroidal Systems* ; July 1991

NIFS-103 A. J. Lichtenberg, K. Itoh, S. - I. Itoh and A. Fukuyama, *The Role of Stochasticity in Sawtooth Oscillation* ; Aug. 1991

NIFS-104 K. Yamazaki and T. Amano, *Plasma Transport Simulation Modeling for Helical Confinement Systems;* Aug. 1991

NIFS-105 T. Sato, T. Hayashi, K. Watanabe, R. Horiuchi, M. Tanaka, N. Sawairi and K. Kusano, *Role of Compressibility on Driven Magnetic Reconnection ;* Aug. 1991

NIFS-106 Qian Wen - Jia, Duan Yun - Bo, Wang Rong - Long and H. Narumi, *Electron Impact Excitation of Positive Ions - Partial Wave Approach in Coulomb - Eikonal Approximation* ; Sep. 1991

NIFS-107 S. Murakami and T. Sato, *Macroscale Particle Simulation of Externally Driven Magnetic Reconnection;* Sep. 1991

NIFS-108 Y. Ogawa, T. Amano, N. Nakajima, Y. Ohyabu, K. Yamazaki, S. P. Hirshman, W. I. van Rij and K. C. Shaing, *Neoclassical Transport Analysis in the Banana Regime on Large Helical Device (LHD) with the DKES Code;* Sep. 1991

NIFS-109 Y. Kondoh, *Thought Analysis on Relaxation and General Principle to Find Relaxed State;* Sep. 1991

NIFS-110 H. Yamada, K. Ida, H. Iguchi, K. Hanatani, S. Morita, O. Kaneko, H. C. Howe, S. P. Hirshman, D. K. Lee, H. Arimoto, M. Hosokawa, H. Idei, S. Kubo, K. Matsuoka, K. Nishimura, S. Okamura, Y. Takeiri, Y. Takita and C. Takahashi, *Shafranov Shift in Low-Aspect-Ratio Heliotron / Torsatron CHS* ; Sep 1991

NIFS-111 R. Horiuchi, M. Uchida and T. Sato, *Simulation Study of Stepwise Relaxation in a Spheromak Plasma ;* Oct. 1991

NIFS-112 M. Sasao, Y. Okabe, A. Fujisawa, H. Iguchi, J. Fujita, H. Yamaoka and M. Wada, *Development of Negative Heavy Ion Sources for Plasma Potential Measurement* ; Oct. 1991

NIFS-113 S. Kawata and H. Nakashima, *Tritium Content of a DT Pellet in Inertial Confinement Fusion* ; Oct. 1991

NIFS-114 M. Okamoto, N. Nakajima and H. Sugama, *Plasma Parameter Estimations for the Large Helical Device Based on the Gyro-Reduced Bohm Scaling* ; Oct. 1991

NIFS-115 Y. Okabe, *Study of Au^- Production in a Plasma-Sputter Type Negative Ion Source* ; Oct. 1991

NIFS-116 M. Sakamoto, K. N. Sato, Y. Ogawa, K. Kawahata, S. Hirokura, S. Okajima, K. Adati, Y. Hamada, S. Hidekuma, K. Ida, Y. Kawasumi, M. Kojima, K. Masai, S. Morita, H. Takahashi, Y. Taniguchi, K. Toi and T. Tsuzuki, *Fast Cooling Phenomena with Ice Pellet Injection in the JIPP T-IIU Tokamak;* Oct. 1991

NIFS-117 K. Itoh, H. Sanuki and S. -I. Itoh, *Fast Ion Loss and Radial Electric Field in Wendelstein VII-Λ Stellarator*; Oct. 1991

NIFS-118 Y. Kondoh and Y. Hosaka, *Kernel Optimum Nearly-analytical Discretization (KOND) Method Applied to Parabolic Equations <<KOND-P Scheme>>;* Nov. 1991

NIFS-119 T. Yabe and T. Ishikawa, *Two- and Three-Dimensional Simulation Code for Radiation-Hydrodynamics in ICF*; Nov. 1991

NIFS-120 S. Kawata, M. Shiromoto and T. Teramoto, *Density-Carrying Particle Method for Fluid* ; Nov. 1991

NIFS-121 T. Ishikawa, P. Y. Wang, K. Wakui and T. Yabe, *A Method for the High-speed Generation of Random Numbers with Arbitrary Distributions;* Nov. 1991

NIFS-122 K. Yamazaki, H. Kaneko, Y. Taniguchi, O. Motojima and LHD Design *Group, Status of LHD Control System Design ; Dec. 1991*

NIFS-123 Y. Kondoh, *Relaxed State of Energy in Incompressible Fluid and Incompressible MHD Fluid* ; Dec. 1991

NIFS-124 K. Ida, S. Hidekuma, M. Kojima, Y. Miura, S. Tsuji, K. Hoshino, M. Mori, N. Suzuki, T. Yamauchi and JFT-2M Group, *Edge Poloidal Rotation Profiles of H-Mode Plasmas in the JFT-2M Tokamak ;* Dec. 1991

NIFS-125 H. Sugama and M. Wakatani, *Statistical Analysis of Anomalous Transport in Resistive Interchange Turbulence* ;Dec. 1991

NIFS-126 K. Narihara, *A Steady State Tokamak Operation by Use of Magnetic Monopoles* ; Dec. 1991

NIFS-127 K. Itoh, S. -I. Itoh and A. Fukuyama, *Energy Transport in the Steady State Plasma Sustained by DC Helicity Current Drive* ;Jan. 1992

NIFS-128 Y. Hamada, Y. Kawasumi, K. Masai, H. Iguchi, A. Fujisawa, JIPP T-IIU Group and Y. Abe, *New High Voltage Parallel Plate Analyzer* ; Jan. 1992

NIFS-129 K. Ida and T. Kato, *Line-Emission Cross Sections for the Charge-exchange Reaction between Fully Stripped Carbon and Atomic Hydrogen in Tokamak Plasma*; Jan. 1992

NIFS-130 T. Hayashi, A. Takei and T. Sato, *Magnetic Surface Breaking in 3D MHD Equilibria of l=2 Heliotron* ; Jan. 1992

NIFS-131 K. Itoh, K. Ichiguchi and S. -I. Itoh, *Beta Limit of Resistive Plasma in Torsatron/Heliotron* ; Feb. 1992

NIFS-132 K.Sato and F. Miyawaki, *Formation of Presheath and Current-Free Double Layer in a Two-Electron-Temperature Plasma* ; Feb. 1992